Adsorbate-induced roughening of Si(100) by interactions at steps

R. E. Butera,[1] D. A. Mirabella,[2] C. M. Aldao,[2] and J. H. Weaver[1,*]

[1]*Department of Materials Science and Engineering, University of Illinois at Urbana-Champaign, Urbana, Illinois 61801, USA*

[2]*Institute of Materials Science and Technology (INTEMA), Universidad Nacional de Mar del Plata-CONICET, Juan B. Justo 4302, B7608FDQ Mar del Plata, Argentina*

(Received 6 April 2010; revised manuscript received 14 June 2010; published 19 July 2010)

Through a detailed study of Cl adsorption on Si(100) using scanning-tunneling microscopy, we identified sites at steps where adsorption leads to roughening and the formation of extended pits and regrowth structures. Using the equilibrium occupation probabilities obtained from experiment, we were able to identify first-nearest-neighbor interactions that destabilized the surface and, when included in Monte Carlo simulations, reproduced the observed pit and regrowth structures. These findings force a reevaluation of currently proposed mechanisms for roughening.

DOI: 10.1103/PhysRevB.82.045309 PACS number(s): 61.43.Bn, 68.35.Ja, 68.37.Ef

I. INTRODUCTION

Surface restructuring and roughening induced by even simple adsorbates such as hydrogen, carbon, oxygen, or nitrogen have been well documented for many surfaces.[1–6] Understanding changes in the surface structure are crucial for catalysis and corrosion as they affect phenomena such as chemisorption,[7] diffusion,[8] and recombination and desorption.[9] Moreover, there has been a great deal of interest in the discovery, understanding, and control of self-assembled nanostructures.[10]

Experimental observations notwithstanding, relatively few theoretical studies have focused on the basic mechanisms underlying surface modification induced by adsorption. Zhdanov and Kasemo[11,12] simulated the effects of three basic interactions on roughening temperature. As depicted with a one-dimensional scheme in Fig. 1, these include an adsorbate-adsorbate lateral interaction (E_1) and two types of interactions between the adsorbates and the substrate (E_2 and E_3). Adsorbate-adsorbate interactions, E_1, induce roughening to minimize repulsion between adjacent adsorbates. An adsorbate can also weaken substrate particle interactions among themselves. In terms of modeling, this is indistinguishable from a second-neighbor repulsive interaction between adsorbates and substrate particles, E_2, as both reduce the surface energy when the underlying substrate particle has neighbors. Finally, an adsorbed particle can have a direct attractive lateral interaction with a substrate particle, E_3, favoring step formation. The effects of these interactions on a generic and isotropic substrate have been studied in Ref. 13. The Si(100) surface is ideal for tests of the effects of these interactions on a real surface, both theoretically and experimentally, because of its simple (2×1) reconstruction. It is also one of the most well-studied surfaces and the surface energetics are well known.[14] The adsorption of halogens on Si(100) are known to lead to roughening at relatively low temperature,[15,16] though models of roughening in the submonolayer regime are still unable to account for the formation of large pits and islands seen in experiment.[17]

In this paper, we focus on a surface interaction that had previously been ignored on Si(100), namely, preferential adsorption at rebonded atoms along S_B steps. Using high-resolution scanning tunnel microscope (STM), we first determine the equilibrium distribution of Cl on the Si(100) surface, finding that adsorption favors occupancy of rebonded atoms. This can be interpreted as an attractive interaction that lowers the effective step-formation energy in a similar manner to that reported for CO adsorption on Pt(110).[18] Monte Carlo (MC) simulations that include this attractive interaction succeed in reproducing the general trends in roughening and surface patterns observed in the low-coverage regime while simulations that ignore it have failed.[17]

II. EXPERIMENTAL DETAILS

The experiments were performed in ultrahigh vacuum (base pressure $<5\times10^{-11}$ Torr) using an Omicron STM1 with RHK SPM100 electronics. The Si wafers were p type, B doped to 0.01–0.02 Ω cm, and oriented within 0.5° of (100). Surface cleaning has been described elsewhere.[19] Starting surfaces had point defects that amounted to 0.01–0.02 monolayer (ML), primarily in the form of dimer vacancies. Once cleaned, the surfaces were flash annealed

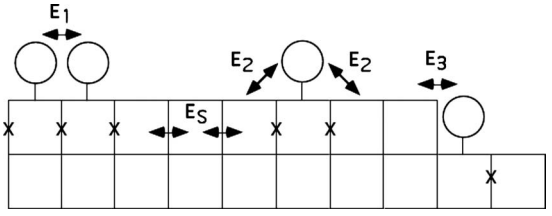

FIG. 1. Schematic of adsorbate-related roughening interactions from Ref. 4. Squares represent substrate particles and circles represent adsorbates. Arrows denote the interactions. E_1 is a repulsive interaction between adsorbates. E_2 is a next-nearest-neighbor adsorbate-substrate interaction that weakens interactions between substrate particles (x's denote weakened E_s interactions). It is equivalent to a repulsive interaction between adsorbates and second neighbors of the substrate. The anticorrelated dimer interaction discussed in the text acts as an attractive interaction E_s between adjacent bare substrate particles. E_3 is a direct nearest-neighbor adsorbate-substrate lateral interaction.

and exposed to Cl_2 at 600 K to minimize water adsorption.[19,20] Annealing at 650 K for 30 s produced the desired equilibrium Cl distribution utilized to determine equilibrium site occupancies. Surfaces were then annealed at 700 K for 2 h to obtain equilibrium pit and island morphologies, for which longer anneal times did not significantly alter pit and island densities or sizes. Gaseous Cl_2 was generated by an electrochemical cell of AgCl doped with 5 wt % $CdCl_2$. A Cl_2 flux of 1.67×10^{-3} ML s^{-1} was used, where 1 ML$=6.78\times10^{14}$ cm^{-2}, the dangling-bond density of Si(100). Filled-state STM images were obtained at room temperature and the Cl concentration was determined by directly counting adsorption sites.[21]

III. MODEL STRATEGY

MC simulations of Si(100) were carried out using a square lattice of 100×100 sites where the surface was modeled as a two-dimensional array of columns of height $h_{i,j}$. A restricted solid-on-solid model was adopted so that overhangs were not allowed, and periodic boundary conditions were used to avoid edge effects. The top of each column represents a substrate particle that was taken to be either a bare dimer or a Cl-terminated dimer. We define the x direction to run from top to bottom and the y direction from left to right of the simulation results. The energy anisotropy of Si(100) was modeled by defining E_x and E_y as the nearest-neighbor interaction perpendicular and parallel to the dimer row direction, and these values alternate between adjacent Si layers so that $E_x^{(h)}=E_y^{(h-1)}$ and $E_y^{(h)}=E_x^{(h-1)}$, where h denotes the Si layer at height h. We adopted substrate interactions of 0.24 eV and 0.05 eV along and across the dimer row direction, respectively, consistent with known step formation energies.[14]

The equilibrium configuration was obtained using the standard method of Metropolis. Two sites i and j were selected at random from an initially flat surface with Cl randomly located. A virtual transfer of a substrate particle i to site j was considered and the energy of the configuration was calculated, and compared to the energy of the initial configuration. If the system gained energy, the exchange was carried out. Otherwise, the exchange was performed with a probability $\exp(-\Delta E/kT)$ where ΔE was a loss of energy ($\Delta E>0$). Next, an adsorbate and a bare site were chosen at random, and the adsorbate was moved to the new site according to the same method as above. The system evolved with successive jumps of substrate particles and adsorbates until it approached the equilibrium configuration. We ensured that the system reached equilibrium by monitoring the evolution of surface roughening. The simulation was ended when the roughness maintained a value within $\pm2\%$ for at least 200 MC times.

IV. RESULTS AND DISCUSSION

Figure 2 is an STM image of Si(100) that had a Cl coverage of 0.23 ML after it was annealed at 700 K for 2 h to reach equilibrium. At this temperature, etching by $SiCl_2$ desorption is negligible but roughening is significant.[15] Although single dimer-wide regrowth chains and vacancy lines can be found scattered about the surface, most have organized into relatively large regrowth islands (I) and vacancy pits (P).

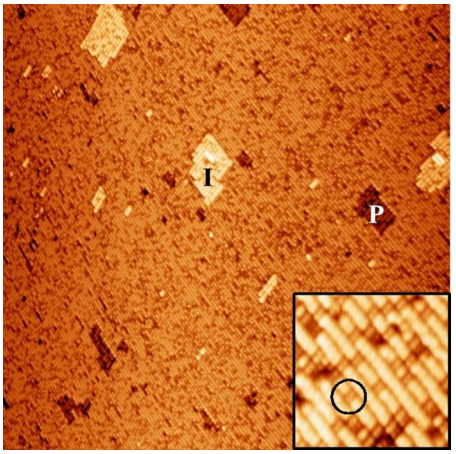

FIG. 2. (Color online) STM image of Si(100) with a Cl coverage of 0.23 ML after annealing at 700 K for 2 h (75×75 nm^2, −3.0 V sample bias). The dimer row direction of the main terrace runs from the upper left to the lower right. Regrowth islands (I) and vacancy pits (P) are generally more than several Si dimer rows in extent. The circle in the inset (6×6 nm^2) highlights a Cl-terminated dimer that is darker in appearance than bare dimers in filled-state images.

Previous MC simulations have failed to reproduce the trend of large and wide features at lower coverage[21] under the currently accepted steric-induced roughening model,[17] where roughening is thought to minimize the repulsion of adjacent adsorbates. The energy gained by keeping the Cl adatoms in isolation offsets that incurred by the introduction of steps. Figure 3(a) shows the results of a MC simulation that included such steric repulsions for the equilibrium configuration with a Cl coverage of 0.3 ML. The x and the y directions of the simulation are labeled, and we have defined S_A and S_B steps associated with pits and islands within the boxed areas. The steric repulsion strengths reported by Boland and coworkers were used (61 meV along the dimers row direction and 26 meV across).[16] Within this model, one would not expect much roughening to occur in the low-coverage regime (<0.5 ML) because there are sufficient bare dimers to avoid neighboring adsorbate-terminated dimers. From Fig. 3(a), the simulation produces a surface where there was limited roughening and what had occurred was due to adsorbate density fluctuations.[17] In contrast to the experimental observation of Fig. 2, the simulated island and pit features were typically 1–2 dimer rows in width. The disagreement with experiment suggests the existence of another interaction that plays a key role in roughening at low coverage.

Chen and Boland[22] addressed roughening in the low-coverage regime by postulating an attractive anticorrelated dimer interaction. In this model, filled dimers would cluster to maximize the amount of adjacent bare buckled dimers. For H-Si(100), this interaction produced "patches" of hydrogen because steric repulsions were negligible. In contrast, the

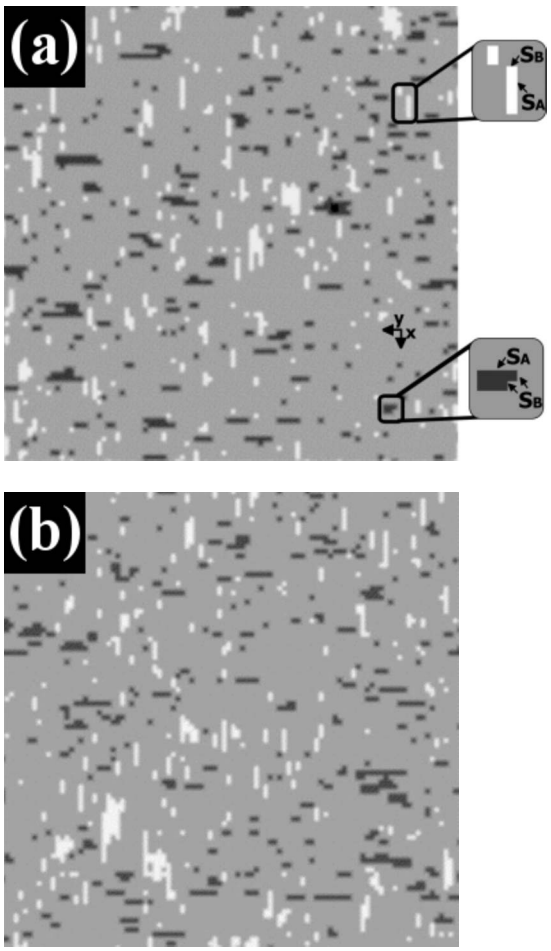

FIG. 3. Monte Carlo outcomes of a 100×100 lattice with 0.3 ML of Cl after reaching equilibrium. Bright features are regrowth and dark features are pits. In (a), *X* and *Y* directions are labeled, and S_A and S_B steps associated with pits and islands are defined. Simulation (a) included steric repulsions of 61 meV along and 26 meV across dimer rows. Simulation (b) included effects of an attractive anticorrelated dimer interaction by considering that the adsorbate distribution was random. Neither (a) nor (b) produced the large islands and pits observed experimentally.

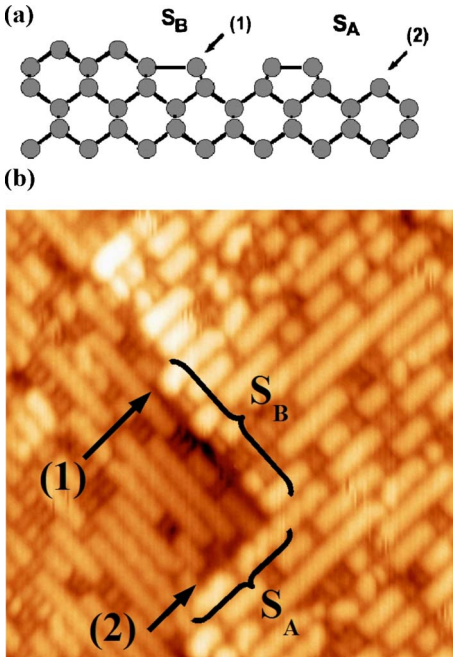

FIG. 4. (Color online) (a) Side view of Si(100) showing S_A and S_B step structures. Atom (1) at the S_B step has shifted to form a long bond that defines the step as being rebonded. (b) STM image of a mixed step that was dominated by rebonded S_B character (12×12 nm^2, -1.2 V). The Cl coverage is 0.13 ML. The distribution of Cl-filled dimers is nearly random on the terrace but examination of the rebonded atom sites reveals that 65% are occupied and appear dark in the image. The chemisorption energy difference between rebonded S_B and terrace sites was found to be 0.14 ± 0.02 eV. Other sites, such as (2) which is close to an S_A step, will have energy differences that are smaller.

much larger Cl atom is randomly distributed since the clustering interaction nearly compensates the steric repulsion. We tested the effect of this anticorrelation interaction by modeling the Cl distribution as random. The steric repulsion values used to generate Fig. 3(a) were compensated by the anticorrelated dimer interaction, and the result is shown in Fig. 3(b). Again, the extent of roughening and the island/pit sizes do not match experiment. We conclude that random Cl distribution consistent with anticorrelation does not substantially increase substrate roughening.

The tendency for adsorbates to cluster, and thus enhance roughening, can be explained by considering Fig. 1. The anticorrelated dimer interaction can be interpreted as an attraction, E_s, between two adjacent bare substrate particles. Disrupted E_s interactions due to adsorbates are labeled with X's. Two adjacent adsorbates will disrupt three E_S interactions while two isolated adsorbates will disrupt four. According to this, adsorption should be favored at sites along steps, at the upper or lower edge since this will disrupt an even fewer number of substrate interactions. When such an interaction was included in MC simulations, we found such a tendency for adsorption at steps. However, experiment shows that Cl is nearly random on the terraces with no preference for upper step edges. One might argue that Cl clustering is then a consequence of a direct attractive interaction between adjacent filled dimers, as suggested for H-Si(100) in Ref. 23. However, the random distribution of Cl on the terraces indicates that the net interaction between Cl-filled dimers is negligible. The fact that roughening occurs, as in Fig. 2, forces us to conclude that another surface interaction is in play.

The key to this new interaction can be found in the Cl distribution at S_B steps, as depicted in Fig. 4(a). For clean and Cl-exposed Si(100), the step is rebonded, with rebonded atoms identified as (1).[24] The STM image of Fig. 4(b) shows a random distribution of Cl on the terrace after Cl_2 exposure at 600 K, to give a coverage of 0.13 ± 0.01 ML, and annealing at 650 K for 30 s. Under these tunneling conditions, the Cl sites are darker than bare sites. Examination of the S_B step reveals Cl attachment to rebonded Si atoms at the base of the step, labeled (1). Hydrogen atoms show a similar tendency to attach at these sites.[25,26]

The equilibrium Cl occupancy of distinct surface sites is related to the difference in adsorption energies. It is assumed that adsorbates do not interact and that the maximum adsorp-

tion is 1 ML. Thus from balance at equilibrium between adsorbates at terrace sites and at rebonded atom sites, we can write

$$\exp\left(\frac{\Delta E}{k_B T}\right) = \frac{\theta_S(1-\theta_T)}{\theta_T(1-\theta_S)}, \quad (1)$$

where k_B is the Boltzmann constant, T is the temperature, and θ_T and θ_S are the Cl occupancies at terraces and steps, respectively. STM images of more than 200 rebonded step sites show that the probability these sites were occupied was 0.65 ± 0.07. Since the probability that a terrace site was occupied was 0.13 ± 0.01, the adsorption energy difference was 0.14 ± 0.02 eV at 650 K. We also observed a different Cl coverage at the lower sites at S_A steps than at terraces, site (2) in Fig. 4(a). This interaction, much weaker than that at S_B steps, could have non-negligible implications on the details of the resulting morphologies. Nevertheless, we only included the influence of the observed preferential adsorption at rebonded step sites in this work to determine if it could produce the type of features observed in Fig. 2.

While oversimplifying, we checked the influence of adsorption at rebonded step sites to determine whether it could yield the features observed in Fig. 2. Preferential adsorption adjacent to a step can be interpreted as an attractive interaction, equivalent to E_3 from Fig. 1, in which the energetics depends solely on the adsorption site occupancy. We stress that the proposed interaction, which we term preferential step adsorption interaction (PSAI), is not a true lateral interaction but this interpretation allows it to be incorporated into MC simulations. The results of incorporating PSAI at S_B steps for a coverage of 0.3 ML are shown in Fig. 5. Comparison to Figs. 3(a) and 3(b) shows that this interaction produced dramatic changes in surface morphology as large pits and islands developed. As a measure of surface disruption, the equilibrium pit areas increased from 5.9% and 6.8% in Figs. 3(a) and 3(b), respectively, to 15.3% in Fig. 5. While the roughness is greater than that determined experimentally, we conclude that the PSAI at steps provide the needed surface processes that previous models could not produce. Even at very low coverage when roughening is expected to be much reduced, PSAI is still present.

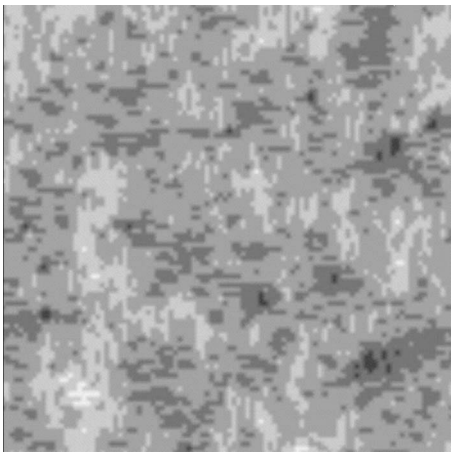

FIG. 5. Monte Carlo simulation (100×100 lattice with 0.3 ML Cl after reaching equilibrium) that included direct adsorbate-substrate lateral interactions of 0.14 eV at S_B steps. In contrast to Fig. 3, this produced large, extended regrowth features and vacancy pits. Comparison to experiment now shows good overall agreement.

While PSAI generates the needed large islands and pits at low coverage, it is clear that adsorption energetics cannot be completely described by considering only first-neighbor interactions. Indeed, the STM images show Cl adsorption close to islands and pits with different probabilities for rebonded atoms within a pit or at the edge of an island. The longer range interactions that account for the Cl populations could have non-negligible implications on the details of roughening, and it is likely that strains related to the formation of dimer rows could also be important in the total island and pit energetics on Si(100). Such finer adjustments are beyond the scope of this paper, the focus of which has been the role of first-nearest-neighbor interactions that provide an important step toward understanding roughening.

ACKNOWLEDGMENTS

This work was supported in part by NSF under Grant No. DMR 0703995. D.A.M. and C.M.A. acknowledge support of the CONICET (Argentina) and the ANPCyT (Grant No. 16-2500, Argentina).

*Corresponding author. FAX: 217-333-2736; jhweaver@illinois.edu

[1] S. Titmuss, A. Wander, and D. A. King, Chem. Rev. **96**, 1291 (1996), and references therein.
[2] *Phase Transitions and Adsorbate Restructuring at Metal Surfaces: The Chemical Physics of Solid Surfaces*, edited by D. A. King and D. P. Woodruff (Elsevier, Amsterdam, 1994), Vol. 7.
[3] R. Stumpf, Phys. Rev. Lett. **78**, 4454 (1997).
[4] L. Hammer, W. Meier, A. Klein, P. Landfried, A. Schmidt, and K. Heinz, Phys. Rev. Lett. **91**, 156101 (2003).
[5] M. J. Harrison, D. P. Woodruff, J. Robinson, D. Sander, W. Pan, and J. Kirschner, Phys. Rev. B **74**, 165402 (2006).
[6] R. Terborg, J. T. Hoeft, M. Polcik, R. Lindsay, O. Schaff, A. M. Bradshaw, R. L. Toomes, N. A. Booth, D. P. Woodruff, E. Rotenberg, and J. Denlinger, Surf. Sci. **446**, 301 (2000).
[7] T. Li, B. Bhatia, and D. S. Sholl, J. Chem. Phys. **121**, 10241 (2004).
[8] D. M. Rampulla, A. J. Gellman, and D. S. Sholl, Surf. Sci. **600**, 2171 (2006).
[9] W. Chen, I. Ermanoski, and T. E. Madey, J. Am. Chem. Soc. **127**, 5014 (2005).
[10] J. Zhang, Z. Wang, J. Liu, S. Chen, and G. Liu, *Self-Assembled Nanostructures* (Kluwer Academic/Plenum, New York, 2003).
[11] V. P. Zhdanov and B. Kasemo, Phys. Rev. B **56**, R10067 (1997).
[12] V. P. Zhdanov and B. Kasemo, J. Chem. Phys. **108**, 4582 (1998).
[13] C. De Micco, S. E. Guidoni, D. A. Mirabella, and C. M. Aldao,

J. Mol. Catal. A: Chem. **228**, 111 (2005).
[14] H. J. W. Zandvliet, Rev. Mod. Phys. **72**, 593 (2000).
[15] K. S. Nakayama, E. Graugnard, and J. H. Weaver, Phys. Rev. Lett. **88**, 125508 (2002).
[16] C. F. Herrmann, D. Chen, and J. J. Boland, Phys. Rev. Lett. **89**, 096102 (2002).
[17] C. M. Aldao, S. E. Guidoni, G. J. Xu, K. S. Nakayama, and J. H. Weaver, Surf. Sci. **551**, 143 (2004).
[18] P. Thostrup, E. Christoffersen, H. T. Lorensen, K. W. Jacobsen, F. Besenbacher, and J. K. Nørskov, Phys. Rev. Lett. **87**, 126102 (2001).
[19] B. R. Trenhaile, A. Agrawal, and J. H. Weaver, Appl. Phys. Lett. **89**, 151917 (2006).
[20] S. Y. Yu, H. Kim, and J. Y. Koo, Phys. Rev. Lett. **100**, 036107 (2008).
[21] G. J. Xu, K. S. Nakayama, B. R. Trenhaile, C. M. Aldao, and J. H. Weaver, Phys. Rev. B **67**, 125321 (2003).
[22] D. Chen and J. J. Boland, Phys. Rev. Lett. **92**, 096103 (2004).
[23] V. P. Zhdanov and P. R. Norton, Langmuir **12**, 101 (1996).
[24] D. J. Chadi, Phys. Rev. Lett. **59**, 1691 (1987).
[25] M. B. Raschke and U. Höfer, Phys. Rev. B **59**, 2783 (1999).
[26] E. Pehlke and P. Kratzer, Phys. Rev. B **59**, 2790 (1999).